# Designing a Glycemic Control Strategy to Maintain Glucose Homeostasis and Prevent Hypoglycemia for Subjects with Type 1 Diabetes

*A. Rafie Lak, O. Vahidi* [*]

*School of Chemical, Petroleum and Gas Engineering, Iran University of Science and Technology, Narmak, P.O. Box: 16846, Tehran, Iran*

| ARTICLE INFO | ABSTRACT |
|---|---|
| | *This paper presents using the fractional $PI^mD^n$ controller module which manipulates insulin infusion rate to maintain normoglycemia in subjects with type 1 diabetes. To prevent severe hypoglycemia, a conventional proportional controller is used to regulate glucagon infusion rate when the blood glucose levels fall below a threshold. Two sets of controller parameters are obtained and evaluated. For the first tuning set, clinical data of an oral glucose tolerance test taken from a group of healthy subjects are used to obtain the controller parameters such that it can mimic a real healthy pancreas. To obtain the second tuning set, the controller parameters are optimized through a sequential quadratic programming algorithm. Using the second tuning set, the in silico 2-hour postprandial test result and comparing it with the glucose concentration trajectory of the healthy subjects show that the controller performs well in returning the blood sugar levels into the glucose homeostasis while keeping the plasma insulin concentration within the acceptable physiological range. It is indicated that the manipulation of glucagon infusion rate is effective in hypoglycemia prevention if more aggressive controller settings are chosen or dysfunctional insulin infusion occurs.* |

## 1. Introduction

Diabetes mellitus is a widespread metabolic disease that affects hundreds of millions in the world. There are two types of diabetes. Type 1 diabetes is an autoimmune disease in which insulin producing cells in the pancreas are destructed leading to a complete halt of insulin secretion. The patients with type 1 diabetes require daily insulin injections to reduce the elevated blood glucose level and maintain it within the physiological range. Type 2 diabetes, on the other hand, is characterized by multiple abnormalities in different body organs resulting in increasing blood sugar levels [1]. Glucose homeostasis in patients with type 2 diabetes can be maintained by suitable dietary program and exercise [2]; however, patients with progressed type 2 diabetes require oral medication and, eventually, insulin injections

to keep the glucose levels in a normal physiological range.

Blood glucose levels are regulated on a negative feedback basis in a healthy human body. Continuous insulin infusion and subcutaneous insulin injections are the two current treatment methods for the insulin-dependent diabetic subjects; due to their inherent open-loop nature, normoglycemia is hardly maintained for the patients [3]. Therefore, to achieve normoglycemia, an alternative treatment method is used to design a device that mimics the closed-loop mechanism of blood glucose regulation in a healthy human body. This device, often referred to as artificial pancreas, has three main components: a mechanical highly accurate pump, an *in vivo* glucose sensor which provides continuous glucose monitoring, and a control module that calculates instantaneous insulin infusion rate based on the measured blood glucose concentration [3, 4].

The risk of severe hypoglycemia, a limiting factor in the glycemic control, is a threat to the insulin-dependent diabetic subjects, which is sometimes fatal [5-7]. Designing a controller strategy that prevents hypoglycemia is vital for the patients. One solution for preventing hypoglycemia is using glucagon infusion whenever the glucose levels drop below a certain threshold [8]. Exogenous glucagon infusion induces more endogenous glucose production which in turn lowers the risk of hypoglycemia. Double purpose pumps which enable delivering both insulin and glucagon together have made this solution practical [9, 10]. Designing a control module for the artificial pancreas based on this solution might be helpful in preventing severe hypoglycemia.

Many studies have been conducted since the early 1970s to design a control algorithm to maintain glucose homeostasis for the insulin-dependent diabetic subjects including conventional PID controller [11-14], sliding mode control [15, 16], model predictive control [17, 18], model-based control [19], robust H control [20, 21], etc. and are reviewed in [22-24]. However, the risk of severe hypoglycemia still remains as an unresolved problem for the designed controllers [25, 26]. In the present study, we have employed a fractional $PI^mD^n$ control module for glycemic control. This controller regulates the blood glucose concentration by adjusting the insulin infusion rate. To avoid hypoglycemia, alongside the insulin loop, another control loop with a conventional proportional (P) controller is utilized for the manipulation of glucagon infusion rate.

To assess the controller performance, we have performed computer simulation using an adjusted mathematical model developed by Vahidi et al. [27] and is presented briefly in the following section. To have the controller mimicking a real healthy pancreas, using a clinical dataset from the healthy subjects group, a set of tuning parameters is obtained for the fractional $PI^mD^n$ controller through solving an optimization problem to generate a glucose concentration trajectory similar to that of the healthy subjects. Another set of the controller tuning parameters is obtained based on integral of time multiplied square error (ITSE) minimization through a sequential quadratic programming algorithm. Comparing the controller response with the response of the glucose regulatory system of the group of healthy subjects shows that the controller is able to regulate the blood sugar level well while keeping the plasma insulin concentration within the physiological range. The risk of severe hypoglycemia is also

reduced by employing glucagon control loop if anything goes wrong with the insulin control loop or more aggressive controller settings are chosen either by intention or by mistake.

## 2. Methodology
### 2.1. Mathematical model

One approach in mathematical modeling of type 1 diabetes mellitus is to select an appropriate model developed for healthy subjects and adjust it for type 1 diabetic subjects. Since the destruction of the pancreatic beta cells is followed by a complete halt of insulin secretion accounts for type 1 diabetes, it is sufficient to use a mathematical model developed for healthy subjects with zero pancreatic insulin secretion rate [4, 28, 29]. The same approach in type 1 diabetes modeling is used by considering the mathematical model developed for healthy subjects and setting its pancreatic insulin secretion rate to zero. Several mathematical models proposed for simulating glucose regulatory system in healthy human subjects started from simple models by Bolie [30] and Ackerman et al. [31] in the early 1960's to more complicated models developed by Cobelli and Mari [32], Sorensen [33], Hovorka et al. [34], and Fessel et al. [35]. The mathematical model used in the present study is an adjusted form of a detailed compartmental model that considers the regulatory hormonal effect of insulin, glucagon, and incretins on blood sugar levels. This model was developed by Vahidi et al. for healthy and type 2 diabetic subjects [27] based on an earlier model by Sorensen [33], which was modified later by Vahidi et al. [36].

The mathematical model comprises four main sub-models, representing blood glucose, insulin, glucagon, and incretins concentrations in the body. In the compartmental modeling approach, the human body is divided into a number of compartments each of which represents a certain organ or a region of the body. Figure 1 depicts the insulin sub-model with seven compartments. Sub-compartments are considered where significant transport resistance between the capillaries and interstitial fluid space exists [33] (e.g., the periphery compartment has two sub-compartments in the insulin sub-model, as shown in Figure 1). The number of compartments differs in each sub-model. The glucose sub-model has the same compartments as the insulin sub-model except for the pancreas compartment not considered as an individual compartment in the glucose sub-model. The whole body is considered as one compartment in the glucagon and incretin sub-models [27]. The mathematical model comprises 27 nonlinear ordinary differential equations resulting from mass balance equations over all sub-compartments. The model equations are available in Appendix.

### 2.2. Fractional $PI^mD^n$ controller

The fractional $PI^mD^n$ controller in Laplace (s) domain has the following form:

$$u(s) = k_c \left(1 + \frac{1}{\tau_i}\frac{1}{s^m} + \tau_d s^n\right) e(s) \qquad (1)$$

where $k_c$, $\tau_i$, and $\tau_d$ are the tuning parameters of the controller proportional, integral, and derivative terms, respectively; $m$ and $n$ are positive fractional numbers, representing the exponent of the integral and derivative terms, respectively; $u(s)$ represents the controller output, and $e(s)$ is the error, given by $e(s) = y_{sp}(s) - y(s)$, with $y_{sp}(s)$ as the desired value of the controlled variable and $y(s)$ as the measured controlled variable.
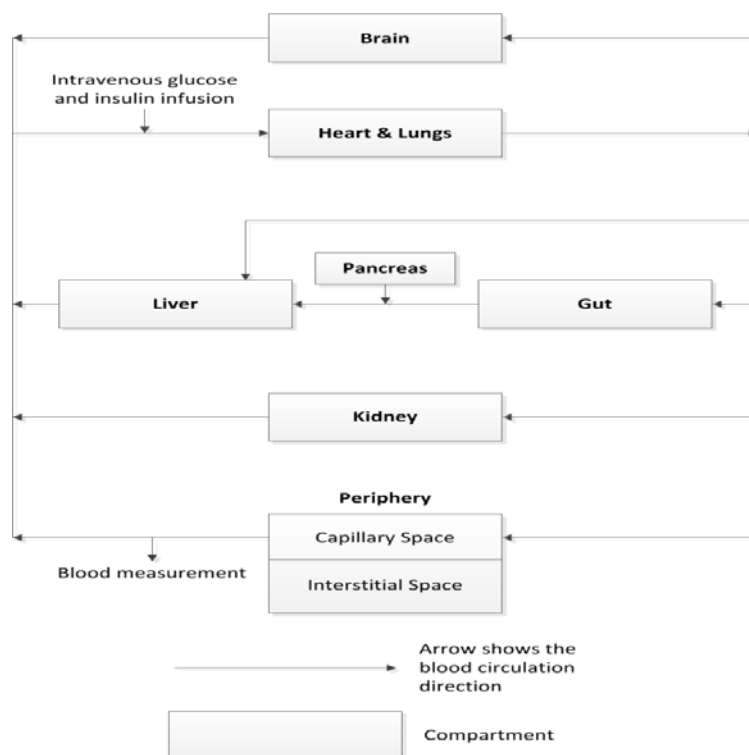
**Figure 1.** Schematic diagram of insulin sub-model. The rectangular blocks represent the sub-model compartments and the arrows indicate blood circulation directions.

Realization of fractional order systems is not trivial. One way to study such systems is through linear approximation. This technique is based on Bode diagrams in frequency domain in which a linear approximation is considered for the fractional order integrator [37, 38]. We have utilized this method for the realization of the fractional $PI^mD^n$ controller briefly described in the following.

Consider the following equation representing a fractional integrator of order *m* in Laplace domain:

$$F(s) = \frac{1}{s^m} \tag{2}$$

The Bode diagram of the above transfer function is characterized by a slope of -20 *m* dB/decade. This line is linearly approximated by a number of connected zig-zag lines with the slopes of 0 dB/decade and -20 dB/decade [37]. For a single-fractal system, the equations representing the linear

approximation of $F(s)$ are:

$$F(s) = \frac{1}{s^m} \approx \frac{1}{\left(1 + \frac{s}{P_T}\right)^m} \approx \frac{\prod_{i=0}^{N-1}\left(1 + \frac{s}{Z_i}\right)}{\prod_{i=0}^{N}\left(1 + \frac{s}{P_i}\right)} \tag{3}$$

$$N = 1 + \text{Integer}\left(\frac{\text{Log}\left(\frac{\omega_{max}}{P_T}\right)}{\text{Log}(ab)}\right) \tag{4}$$

$$a = 10^{y/10(1-m)} \tag{5}$$

$$b = 10^{y/10m} \tag{6}$$

$$P_0 = P_T 10^{y/20m} \tag{7}$$

$$Z_i = P_i a \quad i = 0, ..., N \tag{8}$$

$$P_{i+1} = Z_i b \quad i = 0, ..., N \tag{9}$$

where *y*, in dB, is the discrepancy between the actual line and the linearly approximated lines and $P_T$ is the corner frequency of the transfer function in Eq. (3). $P_T$ and $\omega_{max}$ represent the minimum and maximum frequency ranges

into which the approximation is valid, respectively. The numerical values of the latter two parameters are arbitrarily chosen to cover the desired approximation range.

The described method for fractional integrator approximation is valid when $m$ is at (0, 1] interval. For the larger values of the fractional integrator exponent (i.e., $m>1$), the fractional integrator can be written into the following form:

$$\frac{1}{s^m} = \frac{1}{s^n}\frac{1}{s^\gamma} \tag{10}$$

where $n$ is an integer, and $\gamma$ has a value at (0, 1] interval. The second portion (i.e., $\frac{1}{s^\gamma}$) is linearly approximated by the described method.

## 2.3. The controller structure

To control the blood glucose levels within the normal range, a fractional $PI^mD^n$ controller is employed. The controller acts on the deviation of peripheral glucose concentration (where blood samples are normally taken, indicated in Figure 1) from its desired value by regulating the insulin infusion rate. The desired value for peripheral glucose concentration is considered to be 96 mg/dl. This value corresponds to the healthy subjects' fasting peripheral glucose concentration whose clinical data sets had been collected and used to develop the mathematical model [27]. Since the human body is consuming glucose continuously, it constantly requires insulin. Therefore, a continuous constant insulin infusion rate (i.e., 7.08 mU/min) is considered. This value is calculated such that the peripheral glucose concentrations remain constant under glucose homeostasis condition at 96 mg/dl when no exogenous hydrocarbon is consumed. This value is added to the controller output; hence,

the insulin infusion rate is equal to the summation of this value and the controller output.

In order to prevent severe hypoglycemia, another control loop is utilized which regulates the glucagon infusion rate. This controller also acts on the deviation of peripheral glucose concentration from its desired value. Since no set-point change occurs in blood glucose concentration regulation and no glucagon infusion is desired when the peripheral blood sugar level is above the set-point (i.e., above 96 mg/dl), a simple proportional controller inherently stops glucagon infusion when the blood glucose level is above its set-point suffices for this loop.

Another safety measure for hypoglycemia prevention is to stop infusing insulin when the peripheral blood sugar level falls below a certain threshold considered to be 80 mg/dl. This prevents excessive amount of infused insulin, which may lead to hypoglycemia.

## 3. Results and discussion
### 3.1. Model initialization

As mentioned earlier, the mathematical model comprises 27 nonlinear ordinary differential equations (ODEs). The required initial values for solving the ODEs are obtained from the model's steady-state solution. To find the steady-state solution, the time derivative terms of all ODEs are set to zero and the ODE set turns into a set of nonlinear algebraic equations. Solving the obtained set of equations results in the required initial values for the ODEs. At the steady states, the concentrations of all species and, consequently, all metabolic rates are at basal levels. More details on the steady-state solution are presented in [27].

## 3.2. Mimicking a real healthy pancreas

To have the controller generating a response similar to a real healthy pancreas, the tuning parameters of the fractional $PI^mD^n$ controller are obtained through solving an optimization problem using a clinical data set from a healthy subjects group whose blood sample measurements were used in [27] to estimate the Vahidi et al. model parameters and validate the model results. The data set belongs to a group of ten healthy subjects (two women and eight men) undergone a 50 g OGTT during which 17 blood samples were taken. More details on the used clinical data set is available in [27]. The objective function of the optimization problem is the deviation of the controller response (i.e. the peripheral glucose concentration values from the model) and the glucose concentration levels from the clinical data set, as follows:

$$\min_{\Theta} \sum_{i=1}^{n} \left( G_{PC}{}_m^i - G_{PC}{}_c^i \right)^2 \qquad (11)$$

where $G_{PC}{}_m^i$ is the peripheral glucose concentration from the model at time $i$, $G_{PC}{}_c^i$ is the corresponding glucose concentration from the clinical measurements and $n$ is the number of data points.

Performing an *in silico* 50 g OGTT and solving the optimization problem, two sets of tuning parameters are obtained indicated in Table 1. For the first tuning set, all clinical measurements are considered in Eq. (11) and for the second one, the clinical measurements within the time interval 0 to 100 min are considered (the glucose concentrations of these measurements are above or equal to the glucose concentration desired value). Although the controller with the first tuning set results in a very similar response to the real healthy pancreas (see Figure 2); however, considering all clinical measurements results in a small $\tau_i$, yielding large integral action (see the first tuning set) in comparison with the second tuning set. This large integral action increases the risk of hypoglycemia if higher amount of glucose is consumed. To show this, an *in silico* 75 g OGTT is performed and the results are shown in Figure 3. As this figure shows, a large integral action of the first tuning set results in a large undershoot in the glucose concentration trajectory and a significant increase in the risk of hypoglycemia, while the other tuning set generates a safe glucose concentration profile. Therefore, large integral action should be avoided in tuning the glucose controller setting.
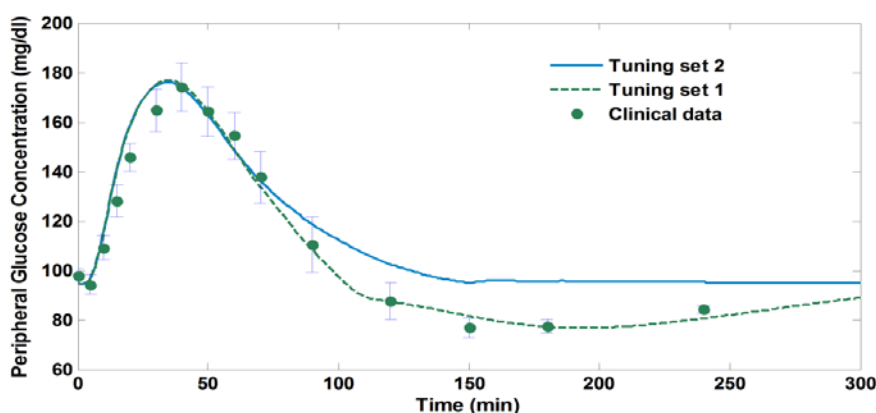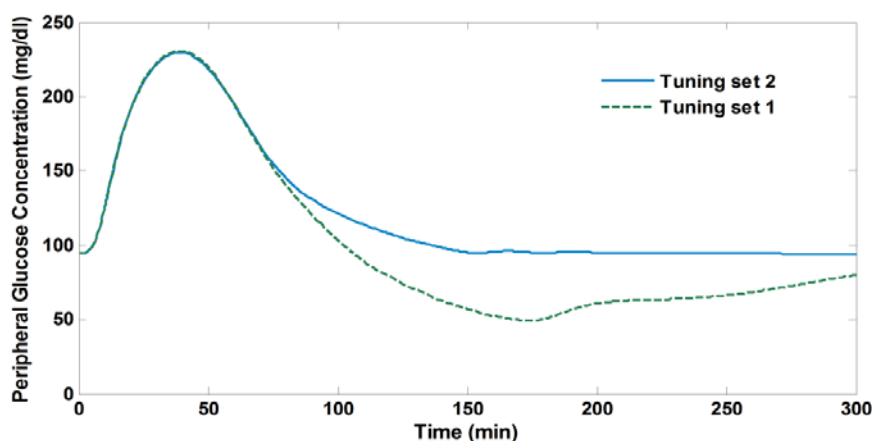


**Figure 2.** Peripheral glucose concentration for an *in silico* 50 g OGTT on diabetic subjects using two controller tuning sets (indicated in Table 1): solid line for the controller with tuning set 2 and dashed line for the controller with tuning set 1. Circles ( ● ) are the results of a 50 g OGTT clinical trial on a group of healthy human subjects.

**Table 1**

Two sets of the fractional $PI^mD^n$ controller tuning parameters.

|  | kc | $\tau_i$ | $\tau_d$ | m | n |
|---|---|---|---|---|---|
| Tuning set 1 | 0.143 | 27.7 | 11.65 | 1.022 | 0.53 |
| Tuning set 2 | 0.187 | 368.8 | 7.37 | 1.175 | 0.42 |



**Figure 3.** Peripheral glucose concentration for an *in silico* 75 g OGTT on diabetic subjects using two controller tuning sets (indicated in Table 1): solid line for the controller with tuning set 2 and dashed line for the controller with tuning set 1.

### 3.3. Controller optimal tuning

Tuning the fractional $PI^mD^n$ controller has been the topic of various studies [39-42]. The tuning method suggested in the literature is mostly based on optimizing the controller parameters by minimizing the integral of absolute error (IAE) [42] or the integral of square error (ISE) [39] for a first-order plus dead time (FOPDT) model of a given system. Several sets of control rules are also provided correlating the controller tuning parameters to the parameters of the FOPDT model.

In the present study, we have used a similar tuning method to find the optimal controller parameters. Due to the availability of the system detailed model, there is no need for the FOPDT model. The system model can be used directly and the controller tuning parameters can be obtained by minimizing the IAE, ISE or other similar objective functions. Here, since reducing the large and prolonged errors are desirable for controlling the blood glucose concentration, the integral of time multiplied square error (ITSE) minimization criterion is selected as the controller tuning method. All programming is done in MATLAB environment.

To find the optimal controller tuning parameters, dynamic simulation of a 50 g oral glucose tolerance test (OGTT) is performed and the controller parameters are tuned by minimizing the ITSE. The obtained controller tuning parameters are shown in Table 2.

**Table 2**

The optimal tuning parameters of fractional $PI^mD^n$ controller.

| Controller | kc | $\tau_i$ | $\tau_d$ | m | n | ITSE |
|---|---|---|---|---|---|---|
| Fractional $PI^mD^n$ | 3.427 | 335.9 | 8.46 | 0.52 | 0.83 | $4.5 \times 10^6$ |

As the controller tuning parameters in Table 2 show, the integral term, $\tau_i$, has a relatively large value which yields poor integration action and slightly affects the controller's response. The reason for the large integral terms is that the controller tuning parameters are obtained by minimizing the ITSE through a load rejection problem (50 g OGTT) where the amount of load is not permanent and its effect on the glucose concentration vanishes eventually by itself. Therefore, only a small integration action is required to eliminate any possible existing error. Furthermore, a large integral action increases the risk of hypoglycemia (discussed in Section 3.5), making its smaller values more desirable.

### 3.4. Controller response assessment

The glycemic controller for a type 1 diabetic subject is supposed to serve as a substitute for the glucose regulatory system of a healthy human subject. Thus, it is relevant to have a comparison between the response of the designed controller and that of a healthy human subject. To do so, dynamic simulation of a 50 g OGTT for a typical healthy human subject is performed using the mathematical model developed by Vahidi et al. [27] (i.e., the same model used in the present study for controlling purposes with nonzero pancreatic insulin secretion). The clinical dataset used in the previous section (by Vahidi et al. [27]) is also indicated.

Figures 4 (a) and (b) show the peripheral glucose and insulin concentration profiles resulting from the dynamic simulation of a 50 g OGTT within which the performance of the fractional $PI^mD^n$ glycemic controller is compared with that of the glucose regulatory system of a typical healthy human subject. As Figure 4 (a) shows, the controller provides a peripheral glucose concentration profile

which falls below the same profile that resulted from the healthy subject's glucose regulatory system. This suggests that using the designed controller strategy guarantees the glycemic control through which the blood glucose concentration remains within the normal physiological range.

Prevention of hyperinsulinemia must be also considered in the insulin therapy. The maximum postprandial physiological level of plasma insulin concentration for a healthy human subject is approximately 170 mU/l [43]; as Figure 4 (b) shows, the peripheral insulin level peak is around 170 mU/l which meets the safety requirements for the physiological insulin level. Although the resulted glucose profile is obtained at the cost of having the insulin concentration profile higher than the profile belonging to the healthy subjects, since the plasma insulin concentration is still within the normal physiological range, the overall controller performance is acceptable. To guarantee keeping the insulin concentration lower than the maximum allowable level, the maximum insulin infusion rate is selected to be 150 mU/min. This value is obtained by dynamic simulation of various values of insulin infusion rate and is implemented for all simulations. It can be adjusted to any other value to guarantee a maximum possible blood insulin concentration.

### 3.5. Glucagon manipulation

To indicate the importance of glucagon manipulation, two scenarios are simulated. In the first scenario, a failure in the insulin control loop is simulated. It is assumed that while the body is resting at glucose homeostasis, the fractional $PI^mD^n$ controller fails to operate and no longer manipulates the insulin infusion rate and a constant rate of

insulin is infused continuously. The constant insulin infusion rate is arbitrarily chosen at 14 mU/min (i.e., approximately twice as big as the normal constant infusion rate). The simulation results are indicated in Figure 5. As Figure 5 (a) shows, when the control loop fails to manipulate the insulin infusion rate and a little higher amount of insulin than the normal continuous rate (i.e., 7.08 mU/min) is infused, the plasma glucose concentration falls below normoglycemia. The higher the continuous infusion rate, the lower the plasma glucose concentration. Continuous infusion of insulin twice bigger than the normal infusion rate causes lowering the peripheral glucose concentration close to 70 mg/dl which is the boundary of hypoglycemia for diabetic subjects [44]. As the simulation results show, a simple proportional controller manipulating glucagon infusion rate is able to keep the plasma glucose concentration within the physiological range by inducing more endogenous glucose production (see Figure 5 (b)). As Figure 5 (b) shows, the hepatic glucose production rate starts from 155 mg/min (i.e., the basal hepatic glucose production rate), and when no glucagon infusion is present, its final value is around 165 mg/min; with glucagon infusion, the final hepatic glucose production rate is around 185 mg/dl which indicates its augmented amount due to the higher plasma glucagon concentration. Although the proportional controller has an intrinsic offset and the utilized controller is not able to return the peripheral glucose concentration exactly to its set-point (i.e., 96 mg/dl), the control loop regulates the glucose level very well and keeps it close enough to its set-point and within the normoglycemia range.
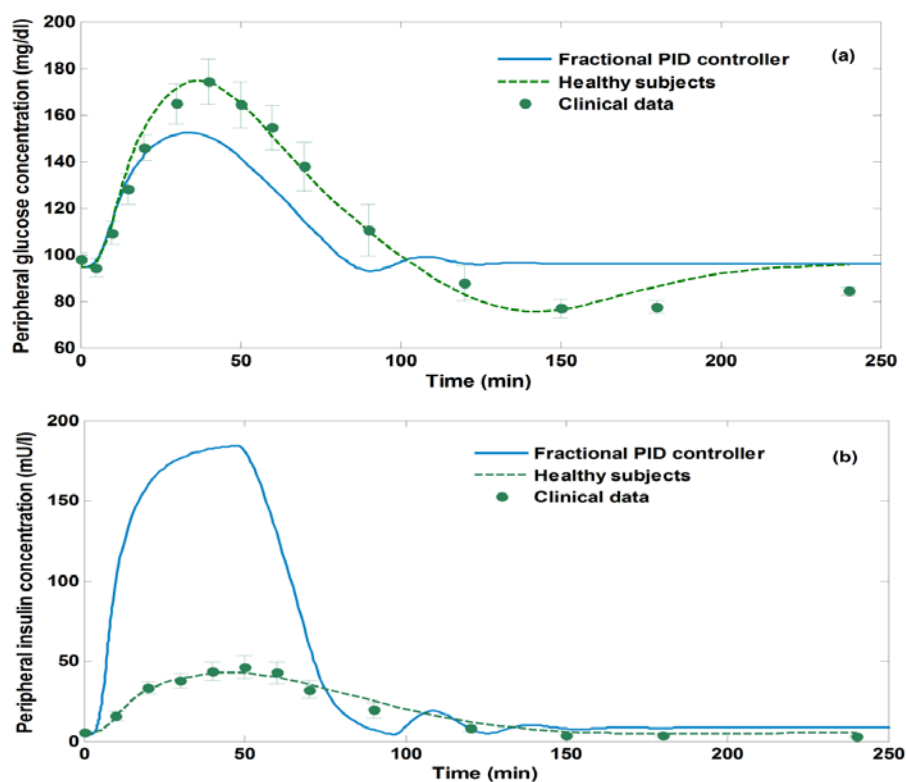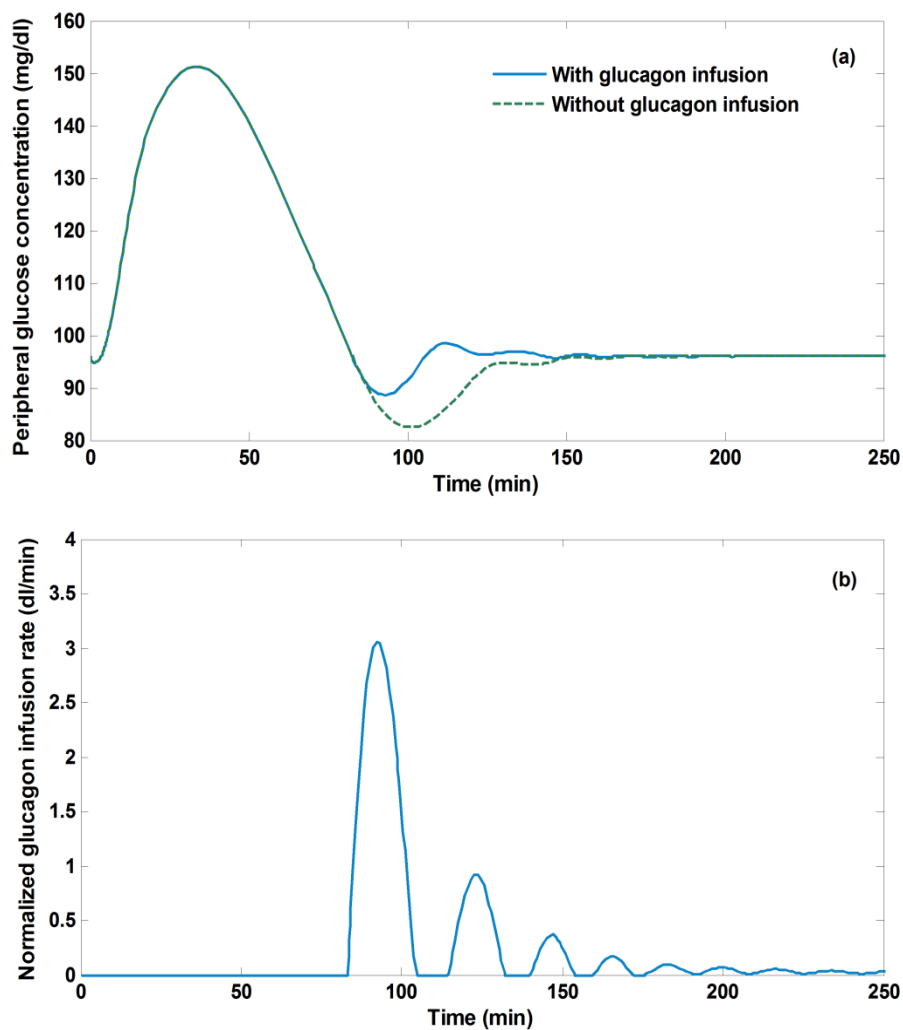


**Figure 4.** Peripheral glucose concentration profile for an *in silico* 50 g OGTT, solid line for the fractional $PI^mD^n$ controller, and dashed line for the glucose regulatory system of a typical healthy subject. Circles (•) are the results of a clinical trial of a 50 g OGTT on a group of healthy human subjects.

In the second scenario, aggressive controller setting is considered (either intentionally or mistakenly). It is assumed that the value of *kc* for the fractional $PI^mD^n$ controller is selected to be twice as big as its optimal value (i.e., 2 x 3.427 = 6.854). In general, higher value of the proportional term results in a more aggressive response; therefore, a large undershoot close to the glucose concentration set-point is expected. Figure 6 shows the results of a 50 g OGTT with the new fractional $PI^mD^n$ controller setting. When the glucagon control loop is off and no glucagon is infused, a big undershoot in blood glucose concentration occurs. Utilizing the glucagon control loop reduces the undershoot amount significantly and maintains the plasma glucose concentration close to its normoglycemia.
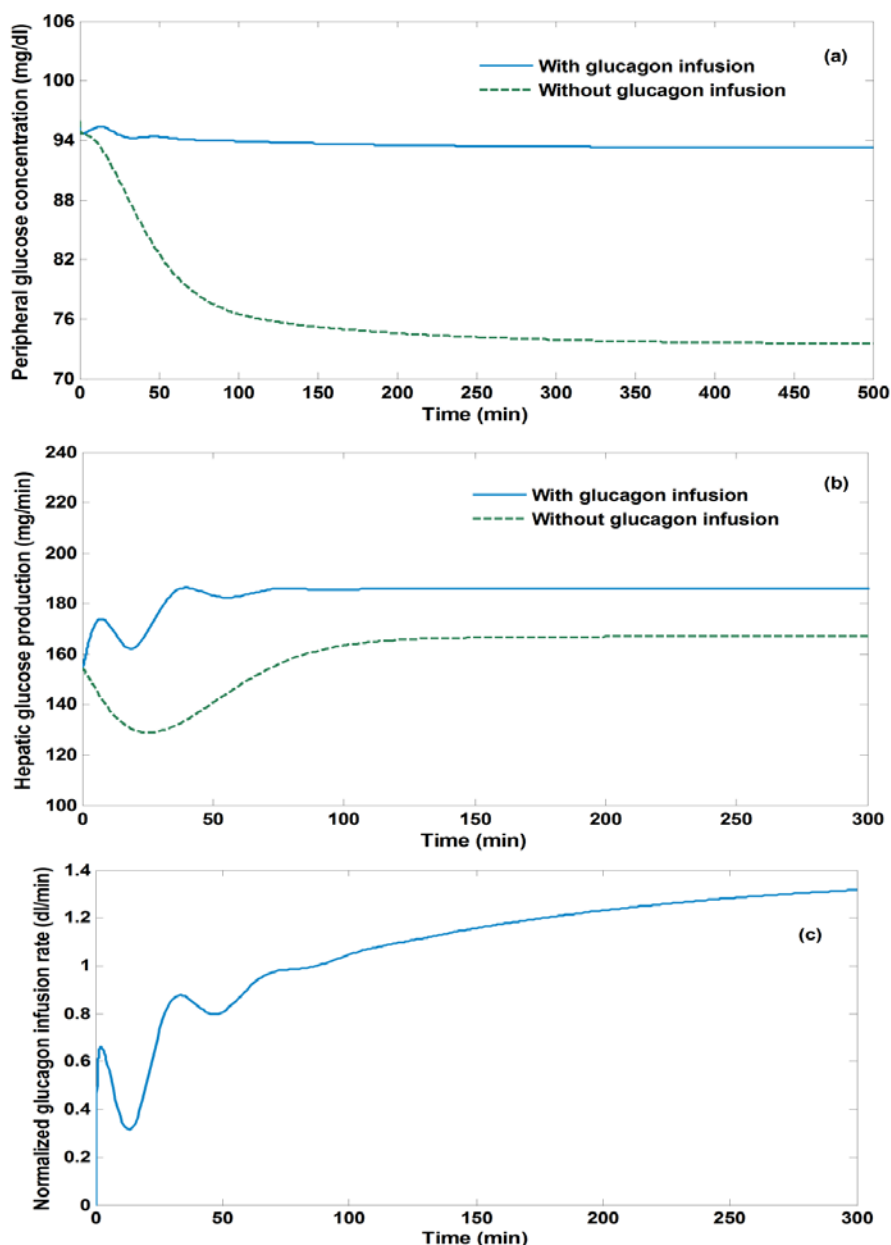


**Figure 5.** The body response following a failure in the insulin control loop (solid line for the presence of exogenous glucagon infusion and dashed line for the absence of exogenous glucagon infusion): (a) peripheral glucose concentration profile, (b) hepatic glucose production profile, and (c) exogenous glucagon infusion rate.

**Figure 6.** The peripheral glucose concentration profile for an in silico 50 g OGTT that resulted from aggressive controller settings, solid line for the presence of exogenous glucagon infusion, and dashed line for the absence of exogenous glucagon infusion.

## 4. Conclusions

In the present study, we employed a fractional $PI^{m}D^{n}$ controller to regulate the plasma glucose concentration of a typical type 1 diabetic subject by manipulating insulin infusion rate. The optimal setting of the controller was obtained by minimizing the integral of time multiplied square error through an *in silico* 50 g OGTT. The controller strategy was assessed by comparing the controller response with the response of the glucose regulatory system of a group of typical healthy subjects, and it was indicated that the controller strategy was able to control the plasma blood concentration within the physiological range while keeping the insulin level below its maximum allowable value; therefore, the strategy could be utilized by an artificial pancreas to control the blood sugar. To have the controller generating a similar glucose concentration trajectory to that of a typical real healthy pancreas, the clinical data set utilized in the controller response assessment was used again to obtain a new set of tuning parameters. It was indicated that the controller was able to provide a similar response to that of the healthy glucose regulatory system. It was shown that a

controller with a moderate integral action should have been chosen to reduce the risk of hypoglycemia. For safety purposes, it was recommended to use the glucagon infusion to avoid hyperglycemia. The effectiveness of this strategy was evaluated by dynamic simulation of two scenarios: one for the fractional $PI^mD^n$ controller failure and one for utilizing more aggressive fractional $PI^mD^n$ controller settings. It was indicated that manipulating the glucagon infusion with a simple proportional controller prevents the risk of hypoglycemia by inducing more endogenous hepatic glucose production which compensates for increased glucose uptake stimulated by excessive level of insulin.

## Nomenclature
### Model variables in the glucose sub-model
| | |
|---|---|
| D | oral glucose amount [mg]. |
| G | glucose concentration [mg/dl]. |
| M | multiplier of metabolic rates. |
| q | glucose amount in GI tract [mg]. |
| Q | vascular blood flow rate [dl/min]. |
| r | metabolic production or consumption rate [mg/min]. |
| Ra | rate of glucose appearance in the blood stream [mg/min]. |
| T | transcapillary diffusion time constant [min]. |
| t | time [min]. |
| V | volume [dl]. |

### Model variables in the insulin sub-model
| | |
|---|---|
| I | insulin concentration [mU/l]. |
| M | multiplier of metabolic rates. |
| r | metabolic production or consumption rate [mU/min]. |
| S | insulin secretion rate [U/min]. |
| T | transcapillary diffusion time constant [min]. |
| t | time [min]. |
| V | volume [dl]. |

### Model variables in the glucagon sub-model
| | |
|---|---|
| $\Gamma$ | normalized glucagon concentration. |
| M | multiplier of metabolic rates. |
| r | normalized metabolic production or consumption rate [dl/min]. |
| V | volume [dl]. |
| t | time [min]. |

### First subscripts
| | |
|---|---|
| $\Gamma$ | glucagon. |
| B | basal condition. |
| G | glucose. |
| I | insulin. |

### Second superscript
| | |
|---|---|
| $\infty$ | final steady state value. |

### Metabolic rate subscripts
| | |
|---|---|
| BGU | brain glucose uptake. |
| GGU | gut glucose uptake. |
| HGP | hepatic glucose production. |
| HGU | hepatic glucose uptake. |
| IVG | intravenous glucose infusion. |
| IVI | intravenous insulin infusion. |
| IV$\Gamma$ | intravenous glucagon infusion |
| KGE | kidney glucose excretion. |
| KIC | kidney insulin clearance. |
| LIC | liver insulin clearance. |
| M$\Gamma$C | metabolic glucagon clearance. |
| P$\Gamma$C | plasma glucagon clearance. |
| P$\Gamma$R | pancreatic glucagon release. |
| PGU | peripheral glucose uptake. |
| PIC | peripheral insulin clearance. |
| PIR | pancreatic insulin release. |
| RBCU | red blood cell glucose uptake. |

### First subscripts
| | |
|---|---|
| A | hepatic artery. |
| B | brain. |
| G | gut. |
| H | heart and lungs. |
| L | liver. |
| P | periphery. |
| S | stomach. |
| $\infty$ | final steady state value. |

### Second subscripts (if required)
| | |
|---|---|
| C | capillary space. |
| F | interstitial fluid space. |
| l | liquid. |
| s | solid. |

## Appendix

## 1. Glucose sub-model

The mass balance equation over each sub-compartment in the glucose sub-model results in following equations:

$$V_{BC}^G \frac{dG_{BC}}{dt} = Q_B^G(G_H - G_{BC}) - \frac{V_{BF}^G}{T_B^G}(G_{BC} - G_{BF}) \tag{1}$$

$$V_{BF}^G \frac{dG_{BF}}{dt} = \frac{V_{BF}^G}{T_B^G}(G_{BC} - G_{BF}) - r_{BGU} \tag{2}$$

$$V_H^G \frac{dG_H}{dt} = Q_B^G G_{BC} + Q_L^G G_L + Q_K^G G_K + Q_P^G G_{PC} - Q_H^G G_H - r_{RBCU} + r_{IVG} \tag{3}$$

$$V_G^G \frac{dG_G}{dt} = Q_G^G(G_H - G_G) - r_{GGU} + Ra \tag{4}$$

$$V_L^G \frac{dG_L}{dt} = Q_A^G G_H + Q_G^G G_G - Q_L^G G_L + r_{HGP} - r_{HGU} \tag{5}$$

$$V_K^G \frac{dG_K}{dt} = Q_K^G(G_H - G_K) - r_{KGE} \tag{6}$$

$$V_{PC}^G \frac{dG_{PC}}{dt} = Q_P^G(G_H - G_{PC}) - \frac{V_{PF}^G}{T_P^G}(G_{PC} - G_{PF}) \tag{7}$$

$$V_{PF}^G \frac{dG_{PF}}{dt} = \frac{V_{PF}^G}{T_P^G}(G_{PC} - G_{PF}) - r_{PGU} \tag{8}$$

The metabolic rates for the glucose sub-model are summarized below:

$$r_{BGU} = 70 \tag{9}$$

$$r_{RBCU} = 10 \tag{10}$$

$$r_{GGU} = 20 \tag{11}$$

$$r_{PGU} = M_{PGU}^I M_{PGU}^G r_{PGU}^B \tag{12}$$

$$r_{PGU}^B = 35 \tag{13}$$

$$M_{PGU}^I = 3.234 + 2.999 \tanh[0.199(I_{PF}/I_{PF}^B - 5.83)] \tag{14}$$

$$M_{PGU}^G = G_{PF}/G_{PF}^B \tag{15}$$

$$r_{HGP} = M_{HGP}^I M_{HGP}^G M_{HGP}^\Gamma r_{HGP}^B \tag{16}$$

$$r_{HGP}^B = 35 \tag{17}$$

$$\frac{d}{dt} M_{HGP}^I = 0.04(M_{HGP}^{I\infty} - M_{HGP}^I) \tag{18}$$

$$M_{HGP}^{I\infty} = 0.838 - 0.789 \tanh[0.535(I_L/I_L^B - 1.39)] \qquad (19)$$

$$M_{HGP}^{G} = 1.113 - 1.105 \tanh[0.5(G_L/G_L^B - 0.794)] \qquad (20)$$

$$M_{HGP}^{\Gamma} = 2.7 \tanh[0.39\,\Gamma/\Gamma^B] - f \qquad (21)$$

$$\frac{d}{dt}f = 0.0154\left[\left(\frac{2.7\tanh[0.39\,\Gamma/\Gamma^B] - 1}{2}\right) - f\right] \qquad (22)$$

$$r_{HGU} = M_{HGU}^{I} M_{HGU}^{G}\, r_{HGU}^{B} \qquad (23)$$

$$r_{HGU}^{B} = 20 \qquad (24)$$

$$\frac{d}{dt}M_{HGU}^{I} = 0.04(M_{HGU}^{I\infty} - M_{HGU}^{I}) \qquad (25)$$

$$M_{HGU}^{I\infty} = \frac{2.0\tanh[c(I_L/I_L^B - d)]}{2.0\tanh[c(1 - d)]} \qquad (26)$$

$$M_{HGU}^{G} = 6.857 + 6.857\tanh[2.03(G_L/G_L^B - 1.626)] \qquad (27)$$

$$r_{KGE} = 71 + 71\tanh[0.11(G_K - 460)] \qquad 0 \le G_K < 460$$

$$r_{KGE} = -330 + 0.872 G_K \qquad\qquad G_K \ge 460 \qquad\qquad (28)$$

To calculate the amount of glucose absorption in the GI tract, *Ra*, a model proposed by Dalla Man et al. [45] was selected and added to the glucose sub-model in our previous work. The model equations are:

$$\frac{dq_{Ss}}{dt} = -0.0688q_{Ss} + D\delta(t) \qquad (29)$$

$$\frac{dq_{Sl}}{dt} = -k_{empt}q_{Sl} + 0.0688q_{Ss} \qquad (30)$$

$$\frac{dq_{int}}{dt} = -0.421q_{int} + k_{empt}q_{Sl} \qquad (31)$$

$$k_{empt} = \frac{0.0434}{2}\{\tanh[\varphi_1(q_{Ss} + q_{Sl} - 0.82D)] - \tanh[\varphi_2(q_{Ss} + q_{Sl} - 0.00236D)] + 2\} \qquad (32)$$

$$\varphi_1 = \frac{5}{2D(1 - 0.82)} \qquad (33)$$

$$\varphi_2 = \frac{5}{0.0047D} \qquad (34)$$

$$Ra = 0.379q_{int} \qquad (35)$$

where $\delta(t)$ is the impulse function.

## 2. Insulin sub-model

The mass balance equation over the sub-compartments in the insulin sub-model results in the

following equations:

$$V_B^I \frac{dI_B}{dt} = Q_B^I(I_H - I_B) \tag{36}$$

$$V_H^I \frac{dI_H}{dt} = Q_B^I I_B + Q_L^I I_L + Q_K^I I_K + Q_P^I I_{PV} - Q_H^I I_H \tag{37}$$

$$V_G^I \frac{dI_G}{dt} = Q_G^I(I_H - I_G) \tag{38}$$

$$V_L^I \frac{dI_L}{dt} = Q_A^I I_H + Q_G^I I_G - Q_L^I I_L + r_{PIR} - r_{LIC} + r_{IVI} \tag{39}$$

$$V_K^I \frac{dI_K}{dt} = Q_K^I(I_H - I_K) - r_{KIC} \tag{40}$$

$$V_{PC}^I \frac{dI_{PC}}{dt} = Q_P^I(I_H - I_{PC}) - \frac{V_{PF}^I}{T_P^I}(I_{PC} - I_{PF}) \tag{41}$$

$$V_{PF}^I \frac{dI_{PF}}{dt} = \frac{V_{PF}^I}{T_P^I}(I_{PC} - I_{PF}) - r_{PIC} \tag{42}$$

The metabolic rates for the insulin sub-model are summarized below:

$$r_{LIC} = 0.4[Q_A^I I_H + Q_G^I I_G + r_{PIR}] \tag{43}$$

$$r_{KIC} = 0.3 Q_K^I I_K \tag{44}$$

$$r_{PIC} = \frac{I_{PF}}{[\left(\frac{1-0.15}{0.15 Q_P^I}\right) - \frac{20}{V_{PF}^I}]} \tag{45}$$

$$r_{PIR} = 0 \tag{46}$$

## 3. Glucagon sub-model
The glucagon sub-model has one mass balance equation over the whole body as follows:

$$V^\Gamma \frac{d\Gamma}{dt} = r_{P\Gamma R} - r_{P\Gamma C} \tag{47}$$

The metabolic rates for the glucagon sub-model are summarized below:

$$r_{P\Gamma C} = 9.1\Gamma \tag{48}$$

$$r_{P\Gamma R} = M_{P\Gamma R}^G M_{P\Gamma R}^I r_{P\Gamma R}^B \tag{49}$$

$$M_{P\Gamma R}^G = 1.31 - 0.61\tanh[1.06(G_H/G_H^B - 0.47)] \tag{50}$$

$$M_{P\Gamma R}^I = 2.93 - 2.09\tanh[4.18(I_H/I_H^B - 0.62)] \tag{51}$$

$$r_{P\Gamma R}^B = 9.1 \tag{52}$$

## 4. Incretins sub-model

The main role of Incretins hormones in glucose metabolism is stimulating the pancreatic insulin secretion following glucose digestion in the GI tract. Since pancreatic secretion is halted in type 1 diabetic subjects, equations belonging to the incretins sub-model are not usable in type 1 diabetes modeling and are not shown here.

The parameters of the described model are available in [36].

## References

[1] Vahidi, O., Bhushan Gopaluni, R. and Kwok, E., "Detection of abnormalities in type II diabetic patients using particle filters", *Journal of Medical and Biological Engineering*, **35** (2), 188 (2015).

[2] Boden, G., Sargrad, K., Homko, C., Mozzoli, M. and Stein, T. P., "Effect of a low-carbohydrate diet on appetite, blood glucose levels, and insulin resistance in obese patients with type 2 diabetes", *Annals of Internal Medicine*, **142** (6), 403 (2005).

[3] Parker, R. S., Doyle, F. J. and Peppas, N. A., "A model-based algorithm for blood glucose control in type I diabetic patients", *IEEE Transactions on Biomedical Engineering*, **46** (2), 148 (1999).

[4] Ramprasad, Y., Rangaiah, G. P. and Lakshminarayanan, S., "Robust PID controller for blood glucose regulation in type I diabetics", *Industrial & Engineering Chemistry Research*, **43** (26), 8257 (2004).

[5] Cryer, P., "Hypoglycaemia: The limiting factor in the glycaemic management of type I and type II diabetes", *Diabetologia*, **45** (7), 937 (2002).

[6] Cryer, P. E., Davis, S. N. and Shamoon, H., "Hypoglycemia in diabetes", *Diabetes Care*, **26** (6), 1902 (2003).

[7] Fowler, M. J., "Hypoglycemia", *Clinical Diabetes*, **26** (4), 170 (2008).

[8] Weinstock, R. S., "Closing the loop: Another step forward", *Diabetes Care*, **34** (9), 2136 (2011).

[9] El-Khatib, F. H., Russell, S. J., Nathan, D. M., Sutherlin, R. G. and Damiano, E. R., "A bihormonal closed-loop artificial pancreas for type 1 diabetes", *Science Translational Medicine*, **2** (27), 27ra27 (2010).

[10] Castle, J. R., Engle, J. M., Youssef, J. E., Massoud, R. G., Yuen, K. C. J., Kagan, R., *et al.*, "Novel use of glucagon in a closed-loop system for prevention of hypoglycemia in type 1 diabetes", *Diabetes Care*, **33** (6), 1282 (2010).

[11] Weinzimer, S. A., Steil, G. M., Swan, K. L., Dziura, J., Kurtz, N. and Tamborlane, W. V., "Fully automated closed-loop insulin delivery versus semiautomated hybrid control in pediatric patients with type 1 diabetes using an artificial pancreas", *Diabetes Care*, **31** (5), 934 (2008).

[12] Steil, G. M., Palerm, C. C., Kurtz, N., Voskanyan, G., Roy, A., Paz, S., *et al.*, "The effect of insulin feedback on closed loop glucose control", *The Journal of Clinical Endocrinology & Metabolism*, **96** (5), 1402 (2011).

[13] Ekram, F., Sun, L., Vahidi, O., Kwok, E. and Gopaluni, R. B., "A feedback glucose control strategy for type II diabetes mellitus based on fuzzy logic", *The Canadian Journal of Chemical Engineering*, **90** (6), 1411 (2012).

[14] León-Vargas, F., Garelli, F., De Battista, H. and Vehí, J., "Postprandial blood glucose control using a hybrid adaptive PD controller with insulin-on-board limitation", *Biomedical Signal Processing and Control*, **8** (6), 724 (2013).

[15] Garcia-Gabin, W., Vehí, J., Bondia, J., Tarín, C. and Calm, R., "Robust sliding mode closed-loop glucose control with meal compensation in type 1 diabetes mellitus", *IFAC Proceedings Volumes*, **41** (2), 4240 (2008).

[16] Kaveh, P. and Shtessel, Y. B., "Blood glucose regulation using higher-order sliding mode control", *International Journal of Robust and Nonlinear Control*, **18** (4-5), 557 (2008).

[17] Magni, L., Raimondo, D. M., Dalla Man, C., De Nicolao, G., Kovatchev, B. and Cobelli, C., "Model predictive control of glucose concentration in type I diabetic patients: An in silico trial", *Biomedical Signal Processing and Control*, **4** (4), 338 (2009).

[18] Abedini Najafabadi, H. and Shahrokhi, M., "Model predictive control of blood sugar in patients with type-1 diabetes", *Optimal Control Applications and Methods*, **37** (4), 559 (2016).

[19] Palumbo, P., Pizzichelli, G., Panunzi, S., Pepe, P. and De Gaetano, A., "Model-based control of plasma glycemia: Tests on populations of virtual patients", *Mathematical Biosciences*, **257**, 2 (2014).

[20] Ruiz-Velázquez, E., Femat, R. and Campos-Delgado, D. U., "Blood glucose control for type I diabetes mellitus: A robust tracking H∞ problem", *Control Engineering Practice*, **12** (9), 1179 (2004).

[21] Chee, F., Savkin, A. V., Fernando, T. L. and Nahavandi, S., "Optimal H infinity insulin injection control for blood glucose regulation in diabetic patients", *IEEE Trans. Biomed. Eng.*, **52** (10), 1625 (2005).

[22] Chase, J. G., Shaw, G. M., Wong, X. W., Lotz, T., Lin, J. and Hann, C. E., "Model-based glycaemic control in critical care: A review of the state of the possible", *Biomedical Signal Processing and Control*, **1** (1), 3 (2006).

[23] Lunze, K., Singh, T., Walter, M., Brendel, M. D. and Leonhardt, S., "Blood glucose control algorithms for type 1 diabetic patients: A methodological review", *Biomedical Signal Processing and Control*, **8** (2), 107 (2013).

[24] Bequette, B. W., "2- Control in physiology and medicine", in Modelling methodology for physiology and medicine, 2$^{nd}$ ed., E. C. Cobelli, ed., Oxford, Elsevier, pp. 13-44, (2014).

[25] Shalitin, S. and Phillip, M., "Hypoglycemia in type 1 diabetes: A still unresolved problem in the era of insulin analogs and pump therapy", *Diabetes Care*, **31** (Supplement 2), S121 (2008).

[26] Karges, B., Rosenbauer, J., Kapellen, T., Wagner, V. M., Schober, E., Karges, W*., et al.*, "Hemoglobin A1c levels and risk of severe hypoglycemia in children and young adults with type 1 diabetes from Germany and Austria: A trend analysis in a cohort of 37,539 patients between 1995 and 2012", *PLoS Med.*, **11** (10), e1001742 (2014).

[27] Vahidi, O., Kwok, K. E., Gopaluni, R. B. and Knop, F. K., "A comprehensive compartmental model of blood glucose regulation for healthy and type 2 diabetic

subjects", *Medical & Biological Engineering & Computing*, 1 (2015).

[28] Farmer, T. G., Edgar, T. F. and Peppas, N. A., "Effectiveness of intravenous infusion algorithms for glucose control in diabetic patients using different simulation models", *Industrial & Engineering Chemistry Research*, **48** (9), 4402 (2009).

[29] Dua, P., Doyle, F. and Pistikopoulos, E., "Multi-objective blood glucose control for type 1 diabetes", *Medical & Biological Engineering & Computing*, **47** (3), 343 (2009).

[30] Bolie, V. W., "Coefficients of normal blood glucose regulation", *Journal of Applied Physiology*, **16**, 783 (1961).

[31] Ackerman, E., Gatewood, L. C., Rosevear, J. W. and Molnar, G. D., "Model studies of blood-glucose regulation", *The Bulletin of Mathematical Biophysics*, **27**, Suppl: 21 (1965).

[32] Cobelli, C. and Mari, A., "Validation of mathematical models of complex endocrine-metabolic systems: A case study on a model of glucose regulation", *Medical & Biological Engineering & Computing*, **21** (4), 390 (1983).

[33] Sorensen, J. T., "A physiological model of glucose metabolism in man and its use to design and assess improved insulin therapies for diabetes", Dissertation/Thesis, Massachusetts Institute of Technology, (1985).

[34] Hovorka, R., Canonico, V., Chassin, L. J., Haueter, U., Massi-Benedetti, M., Orsini Federici, M.*, et al.*, "Nonlinear model predictive control of glucose concentration in subjects with type 1 diabetes", *Physiological Measurement*, **25** (4), 905 (2004).

[35] Fessel, K., Gaither, J. B., Bower, J. K., Gaillard, T., Osei, K. and Rempala, G. A., "Mathematical analysis of a model for glucose regulation", *Math. Biosci. Eng.*, **13** (1), 83 (2016).

[36] Vahidi, O., Kwok, K. E., Gopaluni, R. B. and Sun, L., "Developing a physiological model for type II diabetes mellitus", *Biochemical Engineering Journal*, **55** (1), 7 (2011).

[37] Charef, A., Sun, H., Tsao, Y. and Onaral, B., "Fractal system as represented by singularity function", *Automatic Control, IEEE Transactions*, **37** (9), 1465 (1992).

[38] Ahmad, W. M. and Sprott, J., "Chaos in fractional-order autonomous nonlinear systems", *Chaos, Solitons & Fractals*, **16** (2), 339 (2003).

[39] Valério, D. and da Costa, J. S., "Tuning of fractional PID controllers with Ziegler–Nichols-type rules", *Signal Processing*, **86** (10), 2771 (2006).

[40] Chen, Y., Bhaskaran, T. and Xue, D., "Practical tuning rule development for fractional order proportional and integral controllers", *Journal of Computational and Nonlinear Dynamics*, **3** (2), 021403 (2008).

[41] Gude, J. J. and Kahoraho, E., "Simple tuning rules for fractional PI controllers", in *Emerging Technologies & Factory Automation, ETFA 2009, IEEE Conference*, pp. 1-8, (2009).

[42] Padula, F. and Visioli, A., "Tuning rules for optimal PID and fractional-order PID controllers", *Journal of Process Control*, **21** (1), 69 (2011).

[43] Thiebaud, D., Jacot, E., Defronzo, R. A., Maeder, E., Jequier, E. and Felber, J.-P., "The Effect of graded doses of insulin on total glucose uptake, glucose oxidation and glucose storage in man", *Diabetes*,

**31** (11), 957 (1982).

[44] NIDDK, *Hypoglycemia*, Available: http://www.niddk.nih.gov/ health-information/health-topics/Diabetes/ hypoglycemia/Pages/index.aspx, (2008).

[45] Dalla Man, C., Camilleri, M. and Cobelli, C., "A system model of oral glucose absorption: validation on gold standard data", *IEEE Transactions on Bio-medical Engineering*, **53** (12 Pt 1), 2472 (2006).